Laboratory experiments on mesoscale vortices interacting with two islands

Claudia Cenedese
Physical Oceanography Department, Woods Hole Oceanographic Institution, Woods Hole, Massachusetts, USA

Claudia Adduce
Dipartimento di Scienze dell'Ingegneria Civile, Università di Roma "RomaTre," Rome, Italy

David M. Fratantoni
Physical Oceanography Department, Woods Hole Oceanographic Institution, Woods Hole, Massachusetts, USA

Received 29 September 2004; revised 8 April 2005; accepted 25 May 2005; published 30 September 2005.

[1] The present study investigates the interaction between a self-propagating cyclonic vortex with two right vertical cylinders and determines the conditions for a vortex to bifurcate into two or more vortices. As in previous studies, after the cyclonic vortex came in contact with a cylinder, fluid peeled off the outer edge of the vortex and a so-called "streamer" went around the cylinder in a counterclockwise direction. Under the right conditions, this fluid formed a new cyclonic vortex in the wake of the cylinder, causing bifurcation of the original vortex into two vortices. In some cases, two streamers formed and went around the two cylinders, each forming a new cyclonic vortex. During the experiments, three parameters were varied: G, the separation between the cylinders; d, the diameter of the incident vortex; and y, the distance of the center of the vortex from an axis passing through the center of the gap between the cylinders. The number of vortices generated by the interaction depends on the ratio G/d and on the geometry of the encounter, which is given by the ratio y/g, where $g = G/2$. An unexpected and revealing result was the formation of a dipole vortex downstream of the two islands for values of $-2 < y/g < 0$, $0.25 \leq G/d \leq 0.4$, and $Re_G > 200$, where $Re_G = U_G G/\nu$ is the Reynolds number and U_G is the maximum velocity of the vortex fluid in the gap. A possible mechanism is that the flow within the vortex was funneled between the two islands, and provided it had a sufficiently high velocity, a dipole formed, much like water ejected from a circular nozzle generates a dipole ring. The formation of a vortex of opposite sign to the incident vortex (i.e., anticyclonic) is in agreement with recent observations of North Brazil Current (NBC) rings interacting with the islands of Saint Vincent and Barbados in the eastern Caribbean. The passage between the islands of Saint Vincent and Barbados has values of G/d of approximately 0.5; hence the laboratory result suggests that both cyclonic and anticyclonic vortices could form downstream of them.

Citation: Cenedese, C., C. Adduce, and D. M. Fratantoni (2005), Laboratory experiments on mesoscale vortices interacting with two islands, *J. Geophys. Res.*, *110*, C09023, doi:10.1029/2004JC002734.

1. Introduction

1.1. Oceanographic Context

[2] Oceanic rings and vortices influence the global-scale environment by transporting anomalous physical and biological properties over large distances and between ocean basins, by causing enhanced stirring and mixing, and by influencing the physical and biogeochemical fluxes between the ocean and atmosphere. Some rings shed by major western boundary currents (e.g., Gulf Stream, Kuroshio, East Australian Current) form in the open ocean and may translate for thousands of kilometers before dissipating. Elsewhere ring and vortex formation and translation are topographically constrained and individual features may survive for only a few months (e.g., Gulf of Mexico Loop Current Eddies). The interaction of vortices with abrupt topographic features such as seamounts, submerged ridges, or islands may result in enhanced and localized transfer of anomalous fluid from the vortex to the surrounding environment. In addition, the interaction could result in the formation of new vortices or complete destruction of the incident vortex. This process has been the subject of several recent investigations. For example, observational, laboratory, and numerical studies have examined the collision of Mediterranean water eddies (Meddies) with seamounts in the eastern subtropical North Atlantic [e.g., *Shapiro et al.*, 1992, 1995; *Richardson and Tychensky*,

0148-0227/05/2004JC002734$09.00

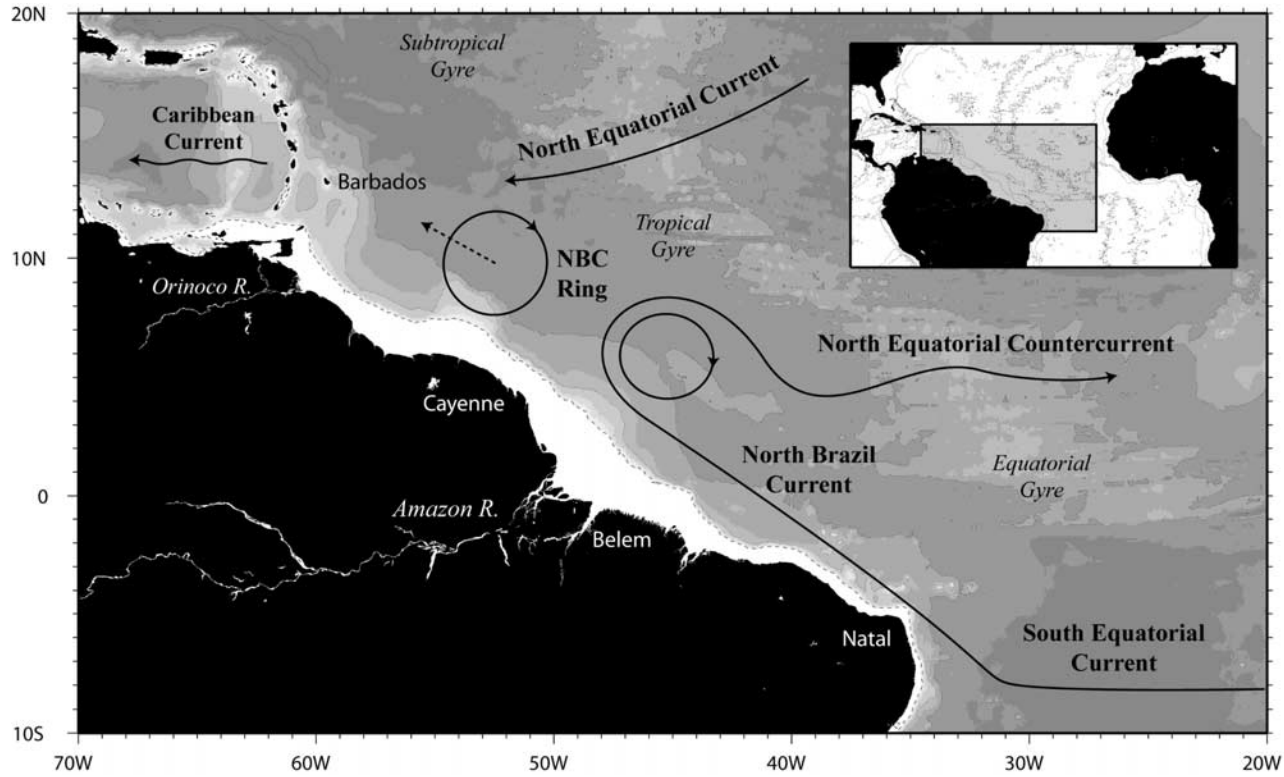

Figure 1. Sketch of the upper ocean circulation in the western tropical Atlantic [from *Fratantoni and Glickson*, 2002].

1998; *Richardson et al.*, 2000; *Simmons and Nof*, 2000; *Cenedese*, 2002; *Wang and Dewar*, 2003; *Adduce and Cenedese*, 2004]. Similar studies have addressed the influence of seamounts and ridges on the evolution of Agulhas rings in the eastern South Atlantic [*Arhan et al.*, 1999; *Schouten et al.*, 2000; *Herbette et al.*, 2003]. The present study has been motivated by a third kind of vortices, North Brazil Current (NBC) rings, that are modified as they encounter the islands of the Lesser Antilles in the western tropical Atlantic. Of great interest is the relationship between NBC rings and a recently documented class of large anticyclonic vortices observed within the eastern Caribbean Sea [*Richardson*, 2005]. In particular, the present study will focus on the interaction of a vortex with two obstacles reproducing, in a very simplified and idealized manner, the scenario in which a NBC ring interacts with the islands of Saint Vincent and Barbados.

[3] Between 6°N and 8°N the North Brazil Current separates sharply from the South American coastline (Figure 1) and curves back on itself (retroflects) to feed the eastward North Equatorial Countercurrent [e.g., *Csanady*, 1985; *Ou and DeRuijter*, 1986; *Garzoli et al.*, 2003]. The NBC occasionally curves back upon itself so far as to pinch off isolated warm-core vortices exceeding 450 km in overall diameter and 2000 m in vertical extent. These NBC rings move northwestward toward the Caribbean at 8–17 cm s^{-1} on a course parallel to the South American coastline while swirling anticyclonically (clockwise) at speeds approaching 100 cm s^{-1} [*Johns et al.*, 1990; *Didden and Schott*, 1993; *Richardson et al.*, 1994; *Fratantoni et al.*, 1995; *Goni and Johns*, 2001; *Fratantoni and Glickson*, 2002; D. M. Fratantoni and P. L. Richardson, The evolution and demise of North Brazil Current rings, submitted to *Journal of Physical Oceanography*, 2005, hereinafter referred to as Fratantoni and Richardson, submitted manuscript, 2005]. Both observations and numerical simulations indicate that most NBC rings turn northward upon reaching the shoaling topography east of the Lesser Antilles and pass very near the island of Barbados. While some numerical simulations and satellite altimeter observations suggest that NBC rings somehow pass intact through the narrow passages of the Lesser Antilles [e.g., *Murphy et al.*, 1999; *Carton and Chao*, 1999; *Goni and Johns*, 2003; *Garraffo et al.*, 2003], the available in situ observations indicate that the rings themselves are destroyed (i.e., lose their coherent vortical circulation) east of the island arc and only filaments of ring core fluid (as identified by Lagrangian drifters) are able to enter the eastern Caribbean Sea (Fratantoni and Richardson, submitted manuscript, 2005).

[4] It has been postulated that the interaction of NBC rings with the Lesser Antilles contributes to the generation of energetic anticyclonic vortices observed downstream of the islands in the eastern Caribbean Sea [*Richardson*, 2005]. These anticyclones have an average diameter of approximately 200 km and translate westward in the central part of the eastern Caribbean Sea. Satellite-tracked drifter observations suggest that in addition to the anticyclones, cyclonic vortices are episodically formed as water accelerates through the narrow passages of the Lesser Antilles [*Richardson*, 2005].

[5] In the present study, we investigate the interaction of a single vortex with two islands. We hypothesize that a vortex interacting with an island pair (or chain) could generate jet-like currents in the island passages resulting in the

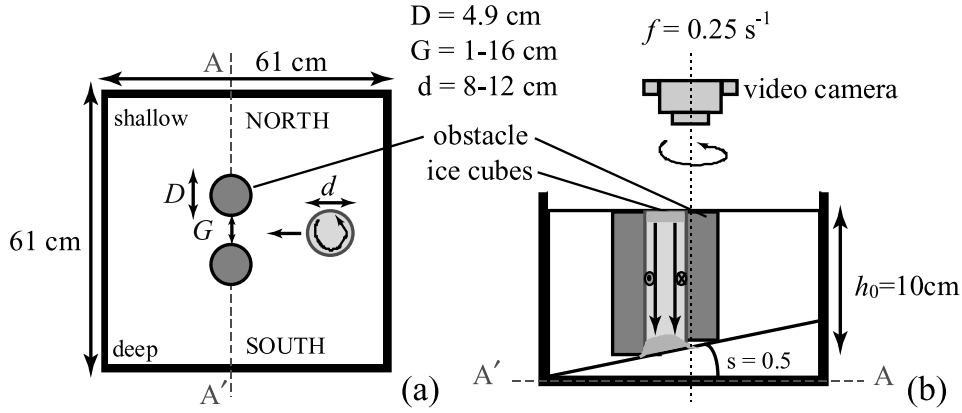

Figure 2. Sketch of the experimental apparatus (not to scale). (a) Top view and (b) side view.

downstream formation of dipole structures. It is expected that these dipoles will have a horizontal dimension smaller than the incident vortex and scale with the passage spacing and/or the island size [*Linden et al.*, 1995]. The fate of such dipoles and how these features can be reconciled with the large, energetic, and predominantly anticyclonic vortices observed by drifters in the eastern Caribbean Sea [*Richardson*, 2005] is a subject under current study.

1.2. Dynamical Background

[6] Only recently have a few studies focused on the interaction of vortices with islands or seamounts and the possibility of "bifurcation" of one vortex into two or more vortices [*Simmons and Nof*, 2000, 2002; *Cenedese*, 2002; *Dewar*, 2002; *Herbette et al.*, 2003; *Wang and Dewar*, 2003; *Adduce and Cenedese*, 2004]. *Simmons and Nof* [2000] analyzed the interaction of a monopolar vortex with a thin wall and found that for a zero potential vorticity lens (with a radius r) to split into two equal lenses, the wall length must be at least $1.19r$. The interaction of a monopolar vortex with a right vertical cylinder was investigated by *Cenedese* [2002]. Both a self-propagating vortex and one advected by a background uniform flow bifurcated into two vortices upon interaction with the cylinder provided $400 \leq Re \leq 1100$, where $Re = v_s d/\nu$ is the Reynolds number, v_s is the velocity of the streamer, and d is the vortex diameter. These values of Re for bifurcation to occur have been established experimentally. This regime corresponds to values of $0.2 \leq R/r \leq 1.0$, for the self-propagating vortex, and $0.2 \leq R/r \leq 1.3$, for the vortex advected by a background flow, where r is the vortex radius and R is the cylinder radius. The difference in the results of these two studies, i.e., bifurcation occurring for $R/r \gtrsim 0.6$ [*Simmons and Nof*, 2000] (for which $2R$ is the wall length) and for $0.2 \leq R/r \leq 1.0$ [*Cenedese*, 2002], could be due to the different geometries used. The interaction of a vortex with a thin wall is different than a vortex interacting with a cylinder; the most striking difference is that in the former case, the horizontal scales have different orders of magnitude, but in the latter case they are the same. Furthermore, in order to better understand the dynamical processes involved when a vortex interacts with seafloor topography, and, in particular, the influence of the topography sloping sidewalls, the topography height and its cross-sectional geometry, a series of idealized laboratory experiments has been performed by *Adduce and Cenedese* [2004]. In particular, the bifurcation mechanism for a vortex interacting with an obstacle having sloping sidewalls (provided the slopes are steep) is similar to the one observed when using vertical sidewalls and the average obstacle diameter is the length scale that should be used in order to collapse the data.

[7] The interaction of both a self-propagating and an advected vortex with multiple islands was recently addressed by *Simmons and Nof* [2002]. The islands were represented by thin vertical walls aligned in the north-south direction with confined passages having a width of 20% of the vortex diameter. Their findings suggest that when the individual islands were small compared to the vortex radius, the vortex reformed in the basin downstream of the islands, while when the islands were large, the vortex broke into smaller vortices. Furthermore, linear quasi-geostrophic theories and modeling of flow through archipelagos [*Pratt and Spall*, 2003] or Rossby normal modes through gaps [*Pedlosky and Spall*, 1999] have shown how the flow or normal modes are able to completely leak through the gaps and reestablish a circulation on the other side. However, the above mentioned numerical models, while explaining some aspects of vortex propagation through small gaps, only treat the linear problem of such interaction. A different picture could result from a laboratory experiment or looking at drifter data in the ocean in which the complete nonlinear problem is tackled or observed.

1.3. Present Study

[8] The laboratory experiments described in the present paper investigated the interaction of a self-propagating vortex with two circular cylindrical islands and we quantitatively classified the different behaviors observed in five different regimes. The paper is organized as follows. In section 2, we describe the apparatus used in the experiments and the measurements taken. In section 3, we describe the phenomena and the evolution of a typical flow in different regimes. In section 4, we compare the results with the prediction by *Cenedese* [2002]. A quantitative description of the dipole formation is given in section 5. Comparisons with observations are made in section 6, and the conclusions of the work are discussed in section 7.

2. Experimental Apparatus

[9] The experiments were conducted in a square tank of depth 36 cm and length and width of 61 cm schematically

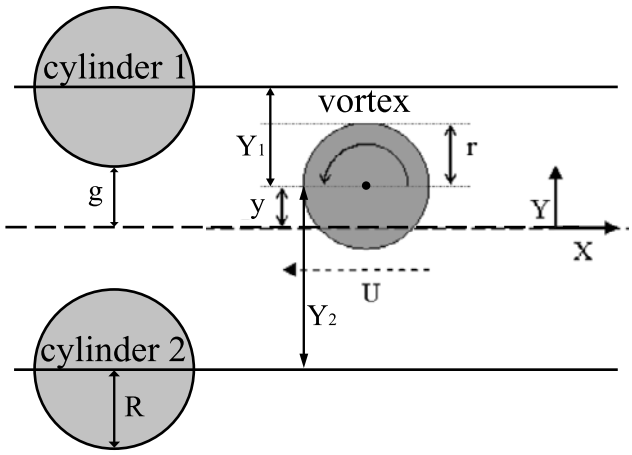

Figure 3. Sketch illustrating the geometry of the encounter between the vortex and two cylinders. The ratio y/g is a measure of the geometry of the interaction. For $y/g > 0$ ($y/g < 0$) the interaction takes place in the northern (southern) side of the gap, and for $y/g = 0$, the interaction is central.

shown in Figure 2. This was mounted concentrically on a 1-m-diameter rotating turntable with a vertical axis of rotation. The sense of rotation of the table was anticlockwise. We used a square tank to avoid optical distortion from side views associated with a circular tank. The tank had a bottom slope, s, in order for the vortex to self-propagate leftward when looking upslope [*Cushman-Roisin*, 1994; *Cenedese and Whitehead*, 2000]. Although the exact equivalence between the sloping topography and the β plane depends on the smallness of the slope and the Rossby number, we will name for reference, north, the shallowest part of the tank. Consequently, east is to the right when looking upslope, west is to the left, and south is the deepest part of the tank. The tank was filled with fresh water, which was initially in solid body rotation. For all the experiments, the depth of the water in the central part of the tank was $h_0 = 10$ cm. The two cylinders were positioned approximately in the central part of the tank as shown in Figure 2. The bottom of each cylinder was sliced at an angle so it rested flush with the sloping bottom.

[10] A barotropic cyclonic vortex was generated by placing an ice cube in the water [*Whitehead et al.*, 1990], a method dynamically similar to withdrawing fluid from a sink positioned on the sloping bottom. The water surrounding the ice cube, because of conduction, became colder than the surrounding water and sank as a cold plume, forming a cold dense lens on the bottom. The inward velocity toward the ice cube, influenced by the Coriolis force, gave rise to cyclonic velocities as showed by paper pallets placed on the free surface. This mechanism makes large and energetic barotropic cyclonic vortices that, after an initial transition period, conserve their properties such as radius and vorticity. The vortex was influenced by the presence of the sloping bottom and self-propagated westward with a very small meridional displacement. Although NBC rings are anticyclonic vortices, in the laboratory we could not reproduce barotropic anticyclones since they tend to be centrifugally unstable [*Kloosterziel and van Heijst*, 1991] and become nonaxisymmetric in a few rotation periods. Furthermore, NBC rings have a baroclinic structure and move within a stratified fluid. (The reader is referred to section 2 of *Adduce and Cenedese* [2004] for a complete discussion on the approximations made in the present model and more details about the vortex generation and drift mechanism.) As discussed by *Cenedese* [2002] and *Adduce and Cenedese* [2004], the use of cyclonic vortices does not limit the generality of the results, which can be easily extended to anticyclones. In particular, the circulation integral arguments in the above mentioned papers, can still be applied to an anticyclonic vortex, the only difference in the results being the sign of the streamer velocity. Consequently the streamer, instead of moving counterclockwise, will go clockwise around the obstacle since the vortex velocity, v_e, for an anticyclone is negative. The condition for bifurcation to occur, $400 \leq Re \leq 1100$, only takes into account the velocity of the streamer; hence it should still hold for anticyclonic vortices. The differences between cyclones and anticyclones in terms of their propagation direction, stability properties, etc., are not investigated in the present paper and the hypothesized mechanism for bifurcation does not rely on any dynamics that are different (a part from the sign) between the two opposite sign vortices.

[11] For all the experiments, the Coriolis parameter f was fixed at 0.25 s^{-1} and the bottom slope was set at $s = \tan\alpha = 0.50$, where α is the angle between the sloping bottom and the horizontal. With this choice of slope magnitude, the self-propagating vortex was observed to move westward with a speed $U \approx 0.2$ cm s^{-1}. The vortex was generated approximately 10 cm westward of the eastern wall and the cylinders' center, positioned in the middle of the tank, was approximately 20 cm westward from the vortex generation site. Hence the vortex moved 20 cm westward and interacted with the cylinders before the spindown time $\tau = h_0/\sqrt{\nu f} = 200$ s. Furthermore, the whole experiment ended when the vortex was approximately 10 cm from the western wall so that the wall effects can be ignored and bottom friction can be neglected. The radii of the cylinders and the vortex are referred to as R and r respectively, as shown in Figure 3. Two circular cylinders were used, with a diameter $D = 2R = 5$ cm. The size of the gap, G, was varied between 1 and 16 cm. The diameter of the vortex, $d = 2r$, was ascertained by observations of particle tracks determined to be within the vortex. Such diameter, d, ranged between 8 and 12 cm and was varied by changing the size of the ice cube. The azimuthal velocity profile of the vortex is similar to that of a Rankine vortex with an approximately constant relative vorticity (solid body rotation) up to a radius $r' = r_{max}$, and then a velocity that decays roughly like $1/r'$, where r'_{max} is the radial coordinate originating in the vortex center. Velocity profile measurements, conducted for some representative experiments, indicated that the measured vortex radius does not correspond to r'_{max}, where the vortex azimuthal velocity is maximum, but is located along the $1/r'$ profile, where the velocity has decayed by approximately 30%. The vortex radius measurements were consistent with this velocity decay definition throughout the experiments and also with the measurements conducted by *Cenedese* [2002] and *Adduce and Cenedese* [2004].

[12] The parameter y, defined as the distance, in the Y direction between the center of the vortex and the horizontal line passing through the center of the gap in the X direction,

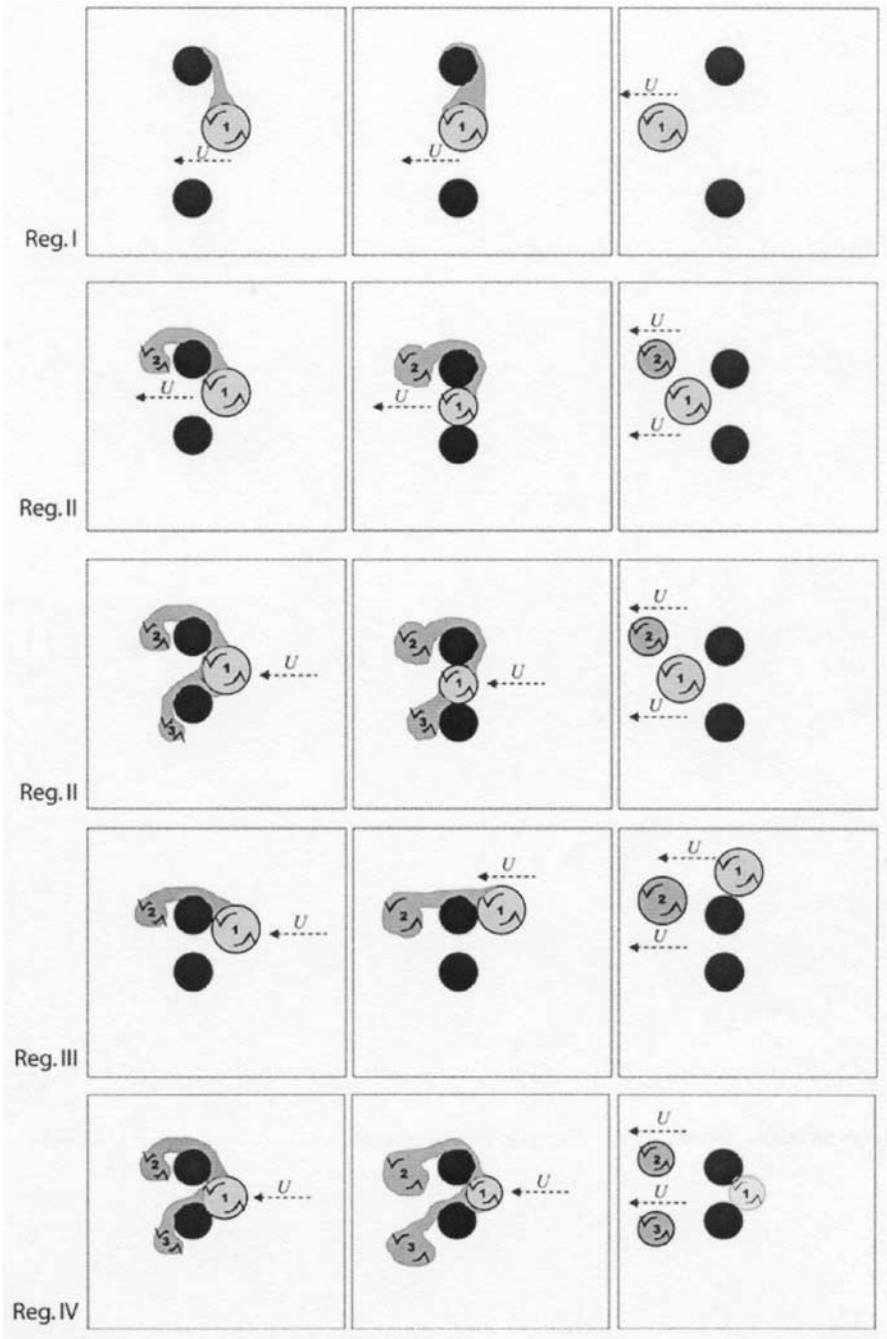

Figure 4. Sketch illustrating a self-propagating cyclonic vortex interacting with two cylinders for four different regimes discussed in section 3. The vortex self-propagated westward at a velocity U indicated by the dashed arrow. The original vortex is indicated by a 1, and the new vortices are indicated by 2 and 3.

represents the geometry of the encounter (Figure 3). This distance was measured just prior to the vortex-cylinders encounter, approximately two vortex diameters upstream of the cylinders. For $y/g > 0$ ($y/g < 0$), the interaction takes place in the northern (southern) side of the gap and for $y/g = 0$, the interaction is central. The parameter y/g was varied between -5 and 5. We will call the cylinder positioned in the northern part of the tank cylinder 1 and the cylinder positioned in the southern part of the tank cylinder 2. Furthermore, Figure 3 illustrates two parameters, Y_1/R and Y_2/R, indicating the geometry of the interaction when considering only cylinders 1 and 2, respectively. As in the work by *Cenedese* [2002], $Y_1(Y_2)$ is defined as the distance in the Y direction between the center of the vortex and the horizontal line passing through the center of cylinder 1 (2) in the X direction.

[13] A video camera was mounted above the tank and fixed to the turntable, in order to observe the flow in the rotating frame. The vortex was made visible by dyeing the ice cube with food coloring and by adding buoyant paper pellets on the free surface. The motion of the dyed vortex was also observed from the side of the tank. The velocities

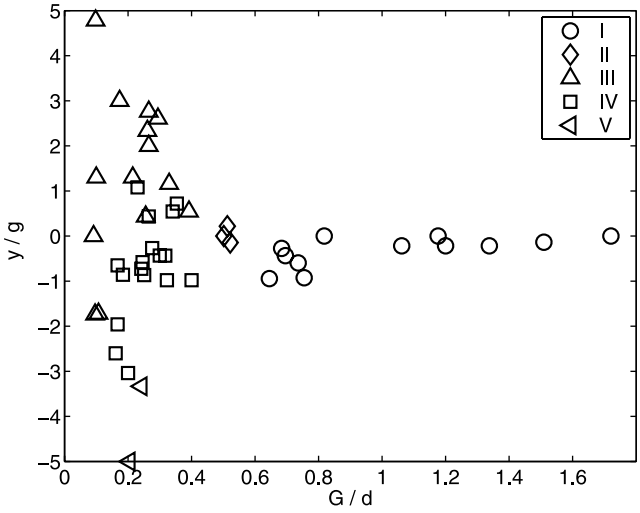

Figure 5. Regime diagram illustrating the values of the parameters G/d and y/g for the five regimes observed for a vortex interacting with two islands.

were measured by tracking the paper pellets on the surface. An image processing software DigImage [*Dalziel*, 1992] was used to acquire and process the images from the videos of the flow. The velocities were obtained by sampling the video at a frequency of approximately 2 Hz. The velocity field was calculated by mapping the individual velocity vectors onto a rectangular grid using a spatial averaging over 3.9 cm, and time averaging over 1.3 s. The vorticity was calculated from this gridded velocity data. The error in the velocities is estimated to be somewhat larger than 5% [*Linden et al.*, 1995], whereas the error in the derived fields is estimated to be approximately 10%.

3. Experimental Results

[14] The experiments have been carried out varying systematically the two geometrical parameters, G/d and y/g, and the results have been classified in five different regimes, which are related to the different dynamics of the vortex-cylinders interaction. Figure 4 illustrates qualitatively the different regimes, while Figure 5 provides the values of the above parameters in the different regimes.

3.1. Regime I: $G/d > 0.6$, No Bifurcation

[15] For values of the ratio $G/d > 0.6$ and all the values of y/g utilized in the experiments, i.e., $-1 < y/g \leq 0$, the cyclonic vortex generated in the eastern side of the tank moved westward over the sloping bottom and through the gap between the two cylinders nearly undisturbed and bifurcation of the original vortex was not observed.

[16] In particular, for $G/d \geq 1.2$, the vortex did not come in contact with any of the cylinders. For $0.75 < G/d < 1.2$, the vortex came in contact with both cylinders, and a small amount of fluid peeled off the outer edge of the vortex and a so-called "streamer" went around cylinder 1 in a counterclockwise direction, as shown schematically in Figure 4. However, the streamer did not generate a new vortex in the wake of cylinder 1, and the original vortex moved westward through the gap. Finally for $0.6 < G/d \leq 0.75$, the fluid from the outer edge of the vortex formed two streamers upon interaction with the two cylinders. Each streamer went around each cylinder in a counterclockwise direction without forming a cyclonic vortex in their wake. As described above, the original vortex moved westward through the gap.

3.2. Regime II: $0.45 < G/d \leq 0.6$, Bifurcation

[17] For values $0.45 < G/d \leq 0.6$ and all the values of y/g utilized in the experiments, i.e., $-0.5 < y/g < 0.5$, the cyclonic vortex came in contact with both cylinders. As described above, the outer part of the vortex formed either one or two streamers that moved counterclockwise around cylinder 1 or each cylinder, respectively. The fluid in the streamer, once it left the cylinder, formed a cyclonic vortex in its wake. Figure 4 illustrates the experiments in which one and two streamers form. In the former case, the original vortex moves through the gap and continues its westward motion independently of the newly formed vortex behind cylinder 1. Hence the final product of a single vortex interacting with two cylinders is two vortices: the original and the newly formed in the wake of cylinder 1. In the case when two streamers form, the original vortex moves through the gap and merges with the vortex forming behind cylinder 2, as shown in Figure 4. It then continues its westward motion along a trajectory approximately parallel to the trajectory of the vortex generated by the streamer in the wake of cylinder 1. Hence the product of the interaction is the same as the case in which only one streamer forms around cylinder 1.

3.3. Regime III: $0 < G/d \leq 0.15$, $0.15 < G/d \leq 0.45$, and $y/g > 1$, Bifurcations

[18] The interaction of a single cyclonic vortex with two cylinders for $0 < G/d \leq 0.15$ and all the values of y/g utilized in the experiments, i.e., $-2 < y/g < 5$, as well for $0.15 < G/d \leq 0.45$ and $y/g > 1$, gives a very similar product as in regime II. The main difference lies in the path followed by the original vortex after the interaction with the two cylinders. The outer part of the vortex formed a streamer only around cylinder 1 and a new cyclonic vortex formed in the wake of the cylinder, as shown in Figure 4. Furthermore, the whole original vortex moved around cylinder 1 counterclockwise and then continued its westward motion somewhat behind the newly formed vortex. Hence the product of the interaction is still two vortices, the original and a newly formed one. However, the original vortex no longer moves through the gap, as in regimes I and II, and instead moves first around cylinder 1 and then westward along a path slightly upslope of the newly formed vortex.

3.4. Regime IV: $0.15 < G/d \leq 0.45$ and $-3 \leq y/g \leq 1$, Bifurcation

[19] For values $0.15 < G/d \leq 0.45$ and $-3 \leq y/g \leq 1$, the cyclonic vortex came in contact with both cylinders and two streamers formed from the outer part of the vortex. Both streamers moved counterclockwise around cylinders 1 and 2 and each formed a new cyclonic vortex in the wake of the cylinders. The original vortex, similar to regime III, was no longer able to move through the gap and it either slowly lost all its fluid to the streamers (Figure 4) or moved as a whole counterclockwise around cylinder 1. In the meantime, the two newly formed vortices moved westward. Hence the

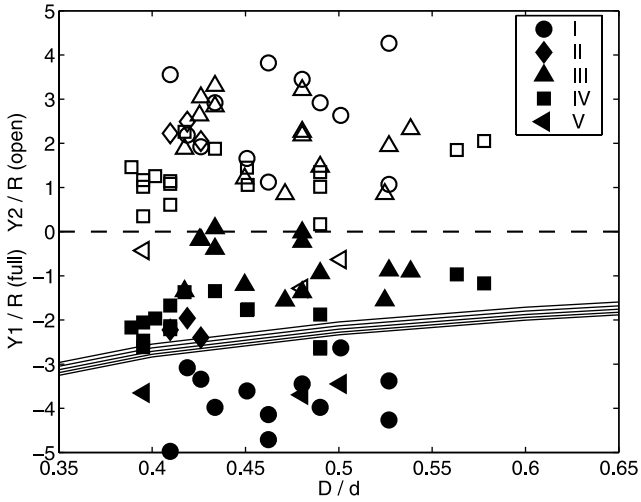

Figure 6. Regime diagram illustrating the parameters used by *Cenedese* [2002] when considering only cylinder 1 (solid symbols) and cylinder 2 (open symbols). Bifurcation should occur between the dashed line and the solid lines.

final product of the interaction was either three vortices, two newly formed and the original vortex, or only two newly formed vortices when the original vortex "died" upstream of the gap between the cylinders (Figure 4). A notable exception to this behavior are two experiments, within this range of values for G/d and y/g, for which a behavior similar to regime III was observed (two triangles in Figure 5 for which $y/g \sim 0.5$ and $0.3 \lesssim G/d \lesssim 0.4$). These two anomalous experiments lie close to the edge between the regime III and the regime IV regions, possibly suggesting that the limits of the regime regions are not sharp.

3.5. Regime V: $0.15 < G/d \leq 0.45$ and $y/g < -3$, Bifurcation

[20] Finally for values of $0.15 < G/d \leq 0.45$ and $y/g < -3$, the cyclonic vortex came in contact only with cylinder 2, and a new cyclonic vortex formed in its wake. The original vortex moved around the southern part of cylinder 2 and continued its westward motion on a path downslope of the newly formed vortex.

4. Discussion

[21] The behavior observed in the five different regimes described above can be explained in light of the results of a previous work conducted by one of the authors investigating the interaction of a cyclonic vortex with a single vertical cylinder [*Cenedese*, 2002]. The results from this previous study will be briefly summarized below, and then we will compare the present results for a cyclonic vortex interacting with two cylinders with these previous results obtained with a single cylinder.

[22] Previous results by *Cenedese* [2002] have shown that bifurcation of a cyclonic self-propagating vortex colliding with a right circular cylinder occurs provided $0.2 \leq D/d \leq 1$, or $400 \leq Re \leq 1100$, and $Y/R \leq 0$. The parameter Y/R described the geometry of the encounter and it is the equivalent of the parameters Y_1/R and Y_2/R described in section 2. After the self-propagating cyclonic vortex came in contact with the cylinder, fluid peeled off the outer edge of the vortex and a streamer went around the cylinder in a counterclockwise direction. Provided the velocity of the streamer, v_s, is large enough, i.e., $Re = v_s d/\nu \geq 400$, the fluid in the streamer will generate a cyclonic vortex in the wake of the cylinder. Hence, for $0.2 \leq D/d \leq 1$ and $Y/R \leq 0$, the fluid in the streamer formed a new cyclonic vortex, while the original vortex passed around the southern part of the cylinder. Consequently, the original vortex bifurcated into two vortices: one containing the original core and the other containing the fluid of the streamer. The physical explanation given by *Cenedese* [2002] for bifurcation occurring only for southern or central interaction ($Y/R \leq 0$) is as follows: for values $Y/R > 0$ (northern interaction), the streamer started forming a new cyclonic vortex in the wake of the cylinder. However, the original vortex passed around the northern side of the cylinder, overtook and merged with the newly formed vortex, and continued its westward drift as a single coherent structure. A different scenario occurred for $Y/R \leq 0$. As before, the streamer formed a new cyclonic vortex in the wake of the cylinder, but the original vortex passed around the southern side of the cylinder, did not overtake the newly formed vortex, and continued its westward drift independent of the new vortex. Meanwhile, the new vortex completed its formation and began drifting westward independent of the original vortex.

[23] During the present experiments, the ratio D/d varied between 0.38 and 0.57. Hence the original cyclonic vortex could bifurcate when interacting with cylinder 1 or/and 2, provided the parameters describing the geometry of the encounter, Y_1/R or/and Y_2/R, are equal or less than zero. Figure 6 illustrates the values of the parameters Y_1/R (solid symbols) and Y_2/R (open symbols) for the five regimes discussed above. The solid curves in the bottom half of Figure 6 represent the lower limit of the parameters, Y_1/R and Y_2/R, for which bifurcation is predicted to occur. They have been obtained for a constant value of the velocity of the vortex fluid along the cylinder, $v_e = 0.5$ cm s^{-1}, and five values of $r = 4.25, 4.75, 5.25, 5.75, 6.25$ cm, corresponding to each curve, since those values are the most representative for the present experiments. For values of Y_1/R and Y_2/R below the solid curves, the vortices are "glancing" the cylinder (i.e., the whole vortex does not interact with the cylinder, but rather with just a peripheral part) and the critical condition for bifurcation ($400 \leq Re \leq 1100$) is not satisfied. The analytical expression for the curves was found by *Adduce and Cenedese* [2004], and the reader is referred to their paper for the analytical derivations and a detailed analysis of glancing interactions. In particular, they provided the following expression for the streamer velocity:

$$v_s = \frac{v_e(\pi - \theta_s)}{\theta_s}, \tag{1}$$

obtained using a circulation integral argument, and where θ_s is defined by the distance, $S_s = R\theta_s$, the streamer travels around the obstacle with an average velocity v_s. The velocity of the vortex fluid along the cylinder outer wall, v_e, is measured, in the laboratory, during the initial stage of the interaction, while the streamer velocity, v_s, is assumed to be constant within and along the obstacle boundary layer, and it is measured along the northern part of the obstacle, just

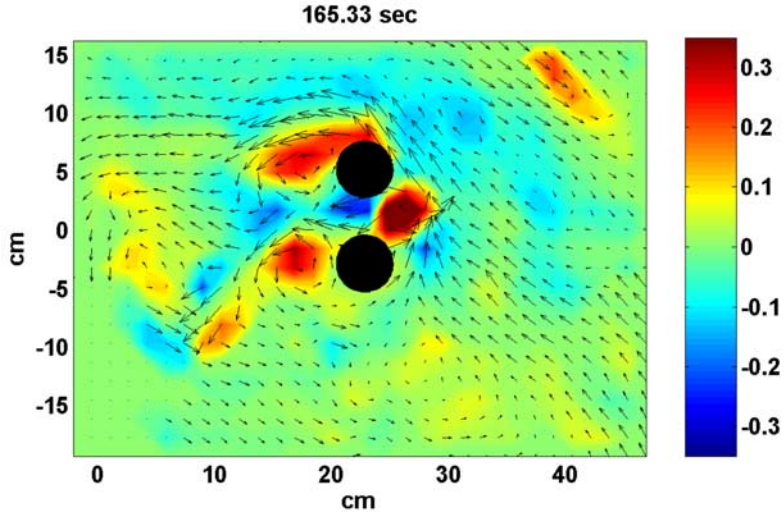

Figure 7. Velocity and vorticity (s^{-1}) fields for an experiment in which a cyclonic vortex forms downstream of cylinders 1 and 2. $G/d = 0.18$ and $y/g = -0.86$.

before the streamer leaves the obstacle. For the present purpose, we assume that bifurcation should occur for values of $0.2 \leq D/d \leq 1$ and $Y_1/R \leq 0$ or/and $Y_2/R \leq 0$ [*Cenedese*, 2002] and for values of Y_1/R or/and Y_2/R, larger than the values of the critical solid curves in Figure 6.

[24] Interactions within regime I did not produce bifurcation of the original vortex because, as shown in Figure 6, the values of Y_2/R were all larger than zero (open symbols) and the values of Y_1/R are below the critical solid curves. Hence bifurcation around cylinder 1 is not expected because the vortex is glancing the cylinder and, although a streamer can form, its velocity, v_s, is not large enough for $Re \geq 400$. Furthermore, although a vortex could form around cylinder 2, since $Y_2/R > 0$, the original vortex overtakes and merges with the newly formed vortex as discussed above, and continues its westward drift as a single coherent structure. Within regime II, bifurcation of the original vortex was observed only to occur around cylinder 1, as predicted by the regime diagram shown in Figure 6. The value of Y_1/R is less than zero, but above the critical solid curves. Hence bifurcation is expected around cylinder 1, while Y_2/R presents always values larger than zero and, as in regime I, a new vortex could form, but it will be overtaken by the original vortex. Figure 6 suggests that within regime III, bifurcation should occur solely around cylinder 1, since Y_1/R is always less or equal to zero and above the critical solid curves, while Y_2/R is larger than zero. Within this regime, bifurcation was indeed observed only around cylinder 1. Bifurcation around cylinder 2 was not observed because of the small distance between the cylinders. It is worth noting that the latter result is not due to the original vortex overtaking the newly formed vortex in the wake of cylinder 2, as in the previous regimes. A streamer around cylinder 2 was either absent, due to $y/g > 1$, or very weak, given the small value of $G/d \leq 0.15$, and the formation of a cyclonic vortex, in the wake of cylinder 2, was not observed. Hence the behavior of a vortex interacting with two cylinders within regime III can be considered equal to a vortex interacting with a single cylinder, extending in the north-south direction.

[25] Figure 6 predicts a very similar behavior for regime IV as for regime III, bifurcation should occur around cylinder 1, since Y_1/R is always less or equal to zero, while it should not occur around cylinder 2, since Y_2/R is larger than zero. However, given the small value of G/d, the original vortex is unable to move undisturbed through the gap. It has been observed to either lose most of its fluid until it can move through the gap, or totally disappear upstream of the gap, or move around cylinder 1. In the wake of cylinder 2, the streamer is able to form a new cyclonic vortex, and this newly formed vortex is undisturbed by the movement of the original vortex and can therefore, move westward as a new independent structure. In the meantime, the streamer around cylinder 1 forms a new vortex, as suggested by Figure 6. Since the original vortex spends a long time in contact with the two cylinders, a large quantity of fluid is withdrawn from it by the streamers and more than one vortex can form in the wake of each cylinder.

[26] Hence the interaction of a single vortex with two cylinders can generate multiple vortices within regime IV. Figure 7 shows the collision between the original vortex and the two cylinders for one such experiment in regime IV. Two streamers move around both cylinders 1 and 2. New vortices form downstream of cylinders 1 and 2, while the original vortex is stalling between the two cylinders and eventually disappears, since all of its fluid has been withdrawn by the new cyclonic vortices.

[27] Finally, Figure 6 indicates that in regime V, bifurcation should not occur around cylinder 1, since the values of Y_1/R are below the critical solid curves; however, bifurcation is expected around cylinder 2, since Y_2/R is less than zero and above the critical solid curves. Again, this prediction is in agreement with the experimental results described in section 3.

5. Dipole Formation

[28] An unexpected and revealing result that occurred in regime IV was the formation of a dipole vortex downstream of the passage between the two islands for values of $-2 <$

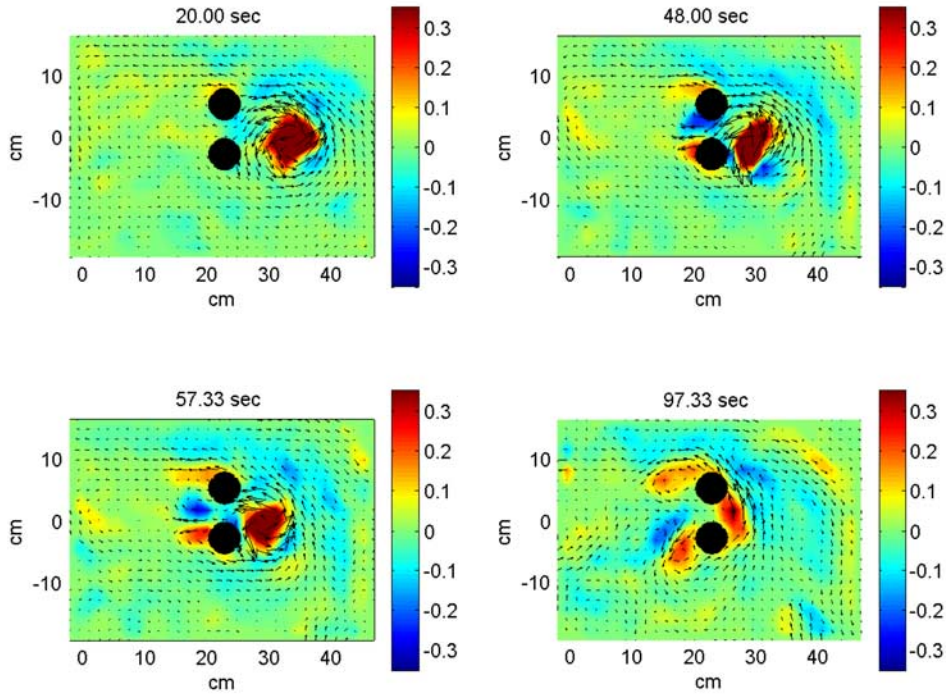

Figure 8. Velocity and vorticity (s^{-1}) fields for an experiment in which dipole formation was observed. $G/d = 0.25$ and $y/g = -0.58$.

$y/g < 0$ and $0.25 \leq G/d \leq 0.4$. The original vortex, generated on the eastern side of the tank, moved westward (Figure 8 at 20 s) and, upon interaction with the two islands, formed a jet passing through the gap as shown in Figure 8 at 48 s with velocities inside the gap almost completely aligned with the X axis; i.e., from east to west. Part of the original vortex fluid formed a streamer around cylinder 1, which formed a new cyclonic vortex in the wake of the cylinder (Figure 8 at 97.33 s). Meanwhile, the fluid from the jet moved through the gap and started forming a dipole structure downstream of it, as shown in Figure 8 at 48 s. The dipole structure is clearly visible in Figure 8 at 57.33 s. The anticyclonic part of the dipole was usually weaker than its cyclonic counterpart, and it was slowly weakened by the presence of the cyclonic vortices around it (Figure 8 at 97.33 s). Hence, although a dipole formation was observed, the anticyclonic vortex weakened and eventually disappeared after approximately 50 s (not shown). Furthermore, in some experiments, the dipole moved southwestward, as shown in Figure 8 at 97.33 s.

[29] A possible mechanism explaining the formation of a dipole upon interaction of a single vortex with two cylinders is as follows: the flow within the vortex is "funneled" between the two islands and, provided this flow has a sufficiently high velocity, a dipole forms, much like water ejected from a circular nozzle generates a dipole ring (for beautiful pictures, see *Van Dyke* [1982]). This scenario is supported by Figure 9, in which the original vortex is dyed and the dipole is clearly visible westward of the two islands.

[30] In order to test the above hypothesis, we measured, for all experiments in regime IV and a few experiments in the other regimes, the temporal evolution of the velocity components u and v, measured between the two islands, the angle γ, the velocity vector of magnitude $U_G = \sqrt{u^2 + v^2}$ forms with the X axis, and the Reynolds number $Re_G = U_G G/\nu$, where $\nu = 0.01$ cm^2 s^{-1} is the kinematic viscosity of water. In particular, u and v were measured where U_G was the maximum velocity within the gap. Figures 10 and 11 show the temporal evolution for the above mentioned variables for two representative experiments: Figure 10, in which dipole formation occurred, and Figure 11, in which it did not. When dipole formation is observed, at approximately $t = 50$ s, the velocity of the fluid passing through the gap is large and directed along the X axis (large u and small v, i.e., small γ) and the corresponding Reynolds number is

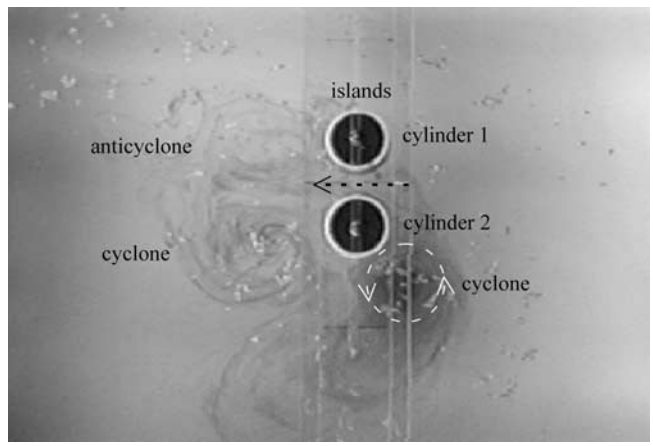

Figure 9. Dipole formation downstream of two islands in an experiment in which the original vortex was dyed.

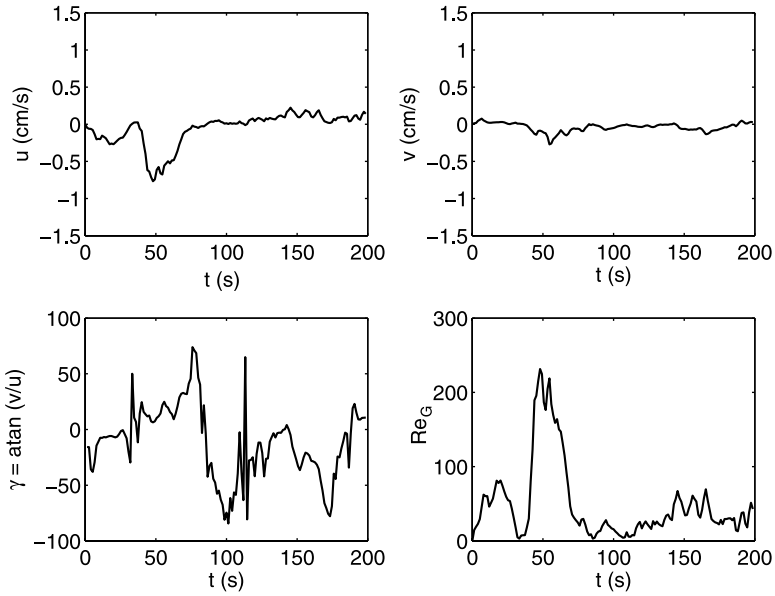

Figure 10. Time series of the velocity components, u and v, the direction of the velocity vector, γ, and the Reynolds number for an experiment with $G/d = 0.3$ and $y/g = -0.43$ in which dipole formation was observed.

also large. In contrast, the velocity of the fluid is small at all times, with a consequent small Reynolds number, for the experiments in which dipole formation was not observed (Figure 11). The cause of the small velocity inside the gap could be one of the following: the gap is too small and the vortex fluid does not pass through the gap ($0 < G/d \leq 0.15$, regime III); the gap is large enough, but most of the vortex fluid moves around cylinder 1 ($0.15 < G/d \leq 0.45$ and $y/g > 1$, regime III and $0.15 < G/d \leq 0.45$, and $-3 \leq y/g \leq 1$, regime IV); the gap is too large and the whole vortex is passing through the gap without forming a jet ($G/d > 0.45$, regimes II and I); or finally some of the vortex fluid may go around cylinder 2 as a streamer but without forming a jet, i.e., without forming an anticyclonic shear on the norther part of the gap ($0.45 < G/d \leq 0.6$, regime II).

[31] Figure 12 shows the maximum value of the Reynolds number during the vortex interaction with the two cylinders, plotted versus y/g. The labels of each symbol indicate the values of the ratio G/d. The open symbols represent the experiments during which no dipole formation was observed, while the solid symbols represent the experiments in which dipole formation occurred. Dipole formation has

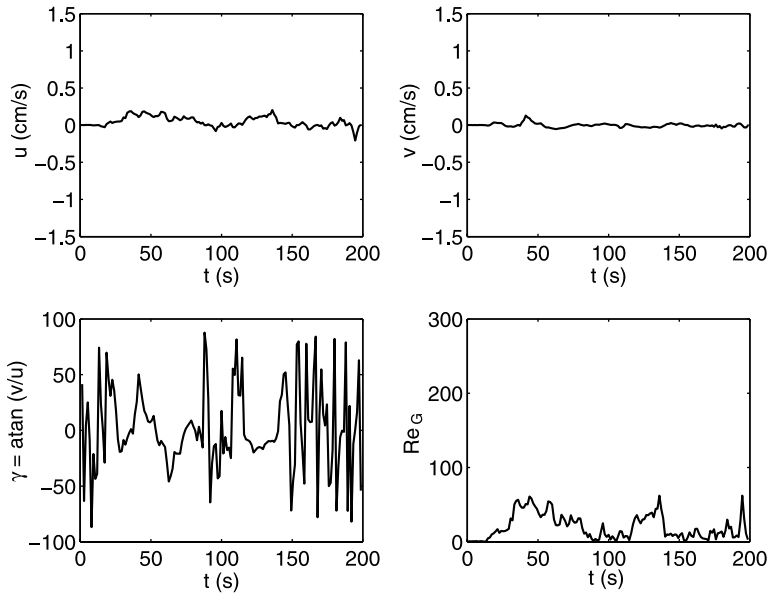

Figure 11. Time series of the velocity components, u and v, the direction of the velocity vector, γ, and the Reynolds number for an experiment with $G/d = 0.29$ and $y/g = 2.6$ in which dipole formation was not observed.

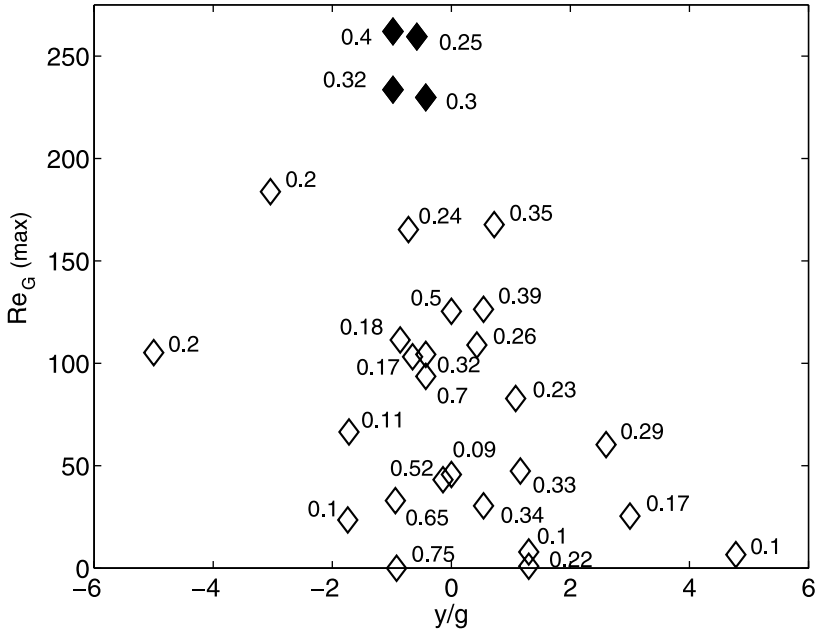

Figure 12. Maximum value of the Reynolds number during the vortex interaction with the two cylinders, plotted versus y/g. Solid (open) symbols indicate experiments in which dipole formation was (was not) observed. The labels of each symbol indicate the values of the ratio G/d.

been observed to occur for $-2 < y/g < 0$ and $0.25 \leq G/d \leq 0.4$ (regime IV), provided the Reynolds number of the fluid ''squeezing'' through the gap reaches values beyond a critical value, $Re_G > 200$, during the interaction.

6. Comparison With Observations

[32] NBC ring translation in the vicinity of the Lesser Antilles is predominantly northward and several rings have been observed to translate through the meridionally oriented passage between the islands of Saint Vincent and Barbados (Fratantoni and Richardson, submitted manuscript, 2005) (Figure 13). The idealized two-island geometry used in the preceding laboratory investigation is loosely modeled on this segment of the Lesser Antilles island arc. The controlling width of this passage is approximately 125 km at the surface, and 80 km at a depth of 1000 m. At depths greater than 1000 m, the western side of this passage is more accurately described as a wall (Figure 13).

[33] Drifters circulating in several NBC rings have been observed to dramatically accelerate northward as the ring passes over or near the island of Barbados. The accelerated fluid exiting the passage between Saint Vincent and Barbados has the characteristics of a jet, with cyclonic and anticyclonic shear zones present on the western and eastern sides, respectively. A particularly compelling example of this behavior is shown in Figure 14, which compares observed drifter trajectories, Figure 14a, with synthetic trajectories, Figure 14b, derived from a laboratory-modeled velocity field. Note that in both cases the drifters on the western side of the passage (bold trajectories in Figure 14) exhibit cyclonic looping, consistent with the expected cyclonic shear on the western side of the jet. Conversely, the drifters on the eastern side of the passage (dashed trajectories in Figure 14) execute one or more anticyclonic loops. The anticyclone formed in the laboratory experiment is poorly sampled: the synthetic drifter looped just once before becoming entrained in the cyclonic portion of the dipole. Note that the laboratory experiment in Figure 14b has the same geometry as described in section 2 and Figure 2. However, Figure 14b has been rotated 90° so that the direction of propagation of the vortex is similar to that of NBC rings, i.e., northward. Furthermore, in order to compare the results obtained in the laboratory with a cyclonic vortex to the NBC anticyclonic rings, one has to remember (section 2) that the streamer of fluid peeling

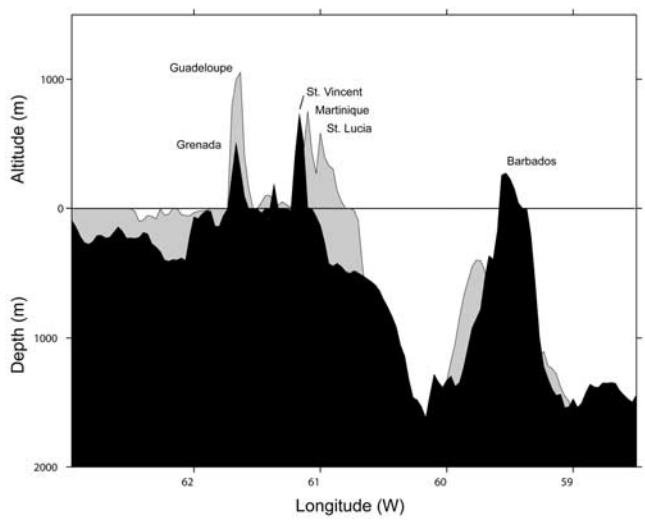

Figure 13. A view of the topography of the eastern Caribbean as seen by an observer looking northward from the island of Tobago. Black indicates the topography along a zonal section through the island of Barbados (approximately 13°N). Gray shows the shallowest topography between 13°N and 20°N.

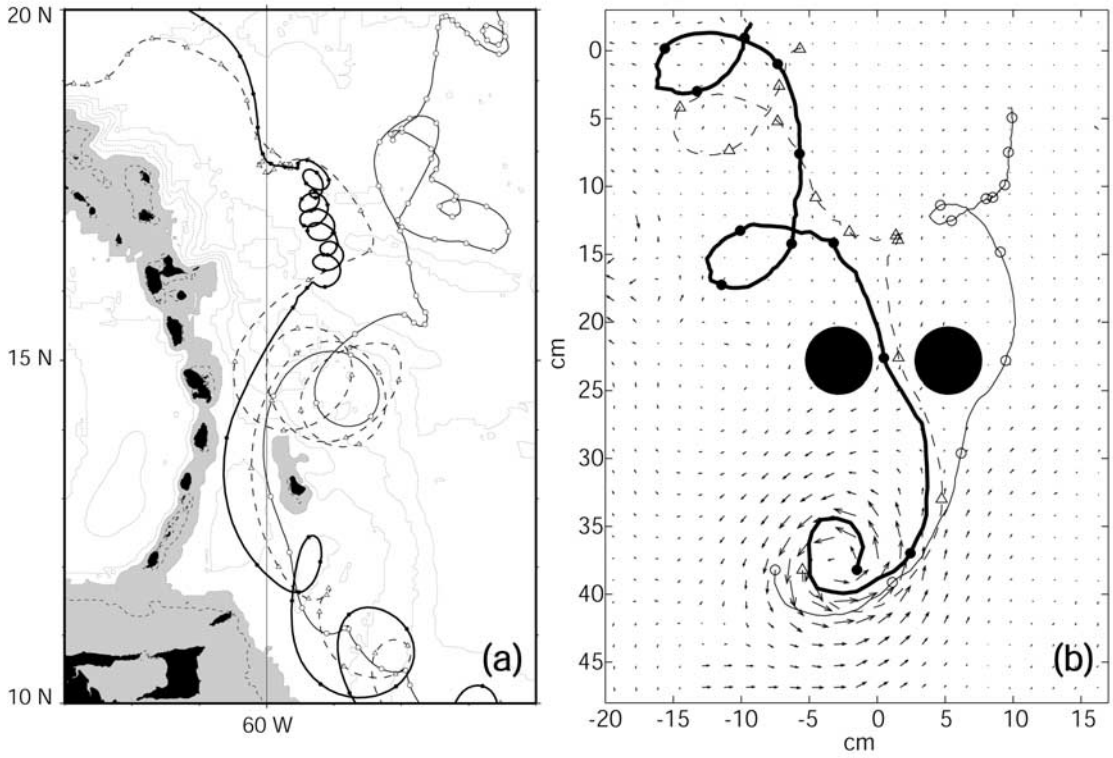

Figure 14. Comparison of (a) observations and (b) laboratory model for a case in which a dipole was observed downstream of the island passage. Shown are trajectories of three satellite-tracked surface drifters in ring 3 (Fratantoni and Richardson, submitted manuscript, 2005) launched in an NBC ring in February 1999 (Figure 14a), compared with three synthetic drifters deployed in the PTV-derived velocity field of the laboratory model (Figure 14b). Areas shallower than 1000 m are shaded. The dashed contour indicates the 200 m isobath. Additional topographic contours appear at 1000 m intervals. Symbols on both sets of trajectories provide a reference for drifter speed and appear at intervals of one inertial period (approximately 2.2 days and 25 s for observations and model, respectively). As described in the text, the sense of rotation for the laboratory eddies is reversed (cyclonic) relative to the observed anticyclonic NBC rings.

off the outer edge of an anticyclonic vortex will go around the obstacle in a clockwise direction.

[34] In the laboratory experiment some fluid moves northward to the east of the island passage. A drifter caught in this flow exhibits a cyclonic tendency (thin trajectory in Figure 14b). As described earlier in the text [see also *Cenedese*, 2002; *Adduce and Cenedese*, 2004], this streamer is a consequence of the cyclonic incident vortex used in the laboratory experiments. Were an anticyclone to approach this passage, our laboratory experiments suggest the streamer would pass inside the gap (i.e., clockwise around Barbados) with no northward flow to the east of the islands. This is consistent with observations which show no evidence of northward flow east of Barbados during an NBC ring encounter (Fratantoni and Richardson, submitted manuscript, 2005).

[35] In the laboratory, formation of dipoles downstream of the island passage was observed for values $0.25 \leq G/d \leq 0.4$ (regime IV). The diameter of the NBC rings reported by Fratantoni and Richardson (submitted manuscript, 2005) varied at the surface between 190 and 330 km with an average value of 250 km while at 1000 m depth, it was reduced to 180 km. Hence G/d for the passage between Saint Vincent and Barbados has surface values $0.38 \leq G/d \leq 0.65$ with an average value of $G/d = 0.5$ while at 1000 m depth $G/d = 0.44$. These values are within or slightly larger than those in regime IV in which dipole formation was observed in the laboratory. The radius of the vortices was determined by eye both for the observations and the laboratory. However, for the observations, the radius corresponded to the position where the azimuthal velocity was maximum while in the laboratory the radius was located where the velocity had decayed by approximately 30% from its maximum value (see section 2). If we were to choose the radius of maximum azimuthal velocity, the laboratory values of the diameter would be smaller and the ratio G/d would be larger. Hence the value of G/d for the oceanographic passage between Saint Vincent and Barbados suggests that both cyclonic and anticyclonic vortices could form downstream of it as observed in Figure 14a.

[36] The other criteria to be satisfied in the laboratory for dipole formation is that the fluid "squeezing" through the gap reaches values of the Reynolds number beyond a critical value, $Re_G > 200$, during the interaction. Determination of the Reynolds number in the ocean is not a trivial task given the uncertainness in the value of the eddy

viscosity. The average velocity of the surface drifters in ring 3 through the passage between Saint Vincent and Barbados (Fratantoni and Richardson, submitted manuscript, 2005) (Figure 14a) is approximately 90 cm s^{-1} while the velocity of the surface drifters in ring 6 through the passage (not shown, for details, see Fratantoni and Richardson (submitted manuscript, 2005)) is 69 cm s^{-1}. Dipole formation was not observed for ring 6, and we are speculating that the reason is the lower velocity of the fluid and, consequently, the lower Re_G given that the passage width and eddy viscosity are the same for both rings. This is only a possible speculation and we are aware that more accurate measurements of the fluid within the passage are necessary to further compare the observations with the laboratory results. If we assume that in the case for which dipole formation was observed (ring 3) the Reynolds number of the fluid in the passage was approximately 200, we would obtain a value of eddy viscosity around 500 m^2 s^{-1} that is of the same order of the value, 300 m^2 s^{-1}, obtained using an eddy-resolving numerical model [*Fratantoni et al.*, 2000], but it is 2 orders of magnitude smaller than the value, $\geq 10^4$ m^2 s^{-1}, obtained using drifters in the region if interest [*Zhurbas and Oh*, 2004].

[37] During the North Brazil Current experiments, only one ring (ring 3) formed a cyclonic vortex (vortex with opposite vorticity than the original ring) after squeezing through the passage between Saint Vincent and Barbados. As discussed above, the absence of a cyclonic vortex could be due to a low velocity of the fluid within the passage. An alternative suggestion is the following: The geometry of the Antilles island chain is different than that used in the laboratory in that the island chain could act as a wall instead of single islands. Hence the formation of cyclonic vortices could be influenced by the presence of the island chain acting as a wall and preventing the formation of cyclonic vortices downstream of the passage. In the laboratory, a different phenomenon could prevent the formation of anticyclonic vortices (vortices with opposite vorticity than the original vortex). As described above, the fluid going northward to the east of the gap (thin trajectory in Figure 14b) forms a cyclonic vortex downstream of the eastern most island and contributes to the destruction, and possibly prevents the formation of anticyclonic vortices downstream of the gap. Hence both in the laboratory and in the ocean, vortices having opposite sign than the incident vortex could be prevented from forming by the presence of other vortices or a "wall-like" topography and not only by a low value of the Reynolds number within the passage.

[38] As a reviewer pointed out, the cyclonic looping of the drifter in Figure 14a started approximately 300 km downstream of Barbados, equivalent to 1.6 diameters of ring 3. On the other hand, the anticyclonic loop in Figure 14b started approximately 6.5 cm downstream of the cylinders, equivalent to 0.65 diameters of the original vortex. We would not expect the laboratory and the real ocean to give exact similar results due to the added complexities in the real ocean such as, for example, the geometric differences discussed above or the presence of background currents. However, the applicability of the laboratory results to the behavior of ring 3 in Figure 14a is only a speculation and it is possible that the cyclonic looping of the drifter in Figure 14a might have been caused by a mechanism different from the one described here.

[39] One of the differences between the present experiments and the real ocean is the slope of the obstacle/island sidewalls. In the laboratory, we used right vertical cylinders; this choice was justified by the earlier work of *Adduce and Cenedese* [2004] showing that the bifurcation mechanism is not influenced by sloping sidewalls, provided the slopes are steep. Furthermore, if we assume that in order to reproduce in the laboratory the dynamics introduced by the sloping sidewalls of an island, the ratio of the relative vorticity of the vortex $\zeta = U'/R'$, where U' and R' are characteristic velocity and length scales, and relative vorticity induced by the sloping topography $\zeta_{topo} = -(fs'R'/H')$, where s' and H' are characteristic slope and depth scales, is the same both in the laboratory experiments and in the ocean, we obtain

$$\frac{U'_{lab}}{\left(\frac{s'f}{H'}\right)_{lab} R'^2_{lab}} = \frac{U'_{oce}}{\left(\frac{s'f}{H'}\right)_{oce} R'^2_{oce}}. \quad (2)$$

NBC rings have a drift velocity of $\sim$15 cm s^{-1} and a radius of approximately 100 km. The sloping walls of a seamount are typically $s'_{oce} \approx 0.04$, while $f \approx 10^{-4}$ s^{-1} and $H'_{oce} \approx$ 1000 m. In the laboratory, $U'_{lab} \approx 0.2$ cm s^{-1}, $R'_{lab} \approx 5$ cm, $f = 0.25$ s^{-1} and $H'_{lab} = h_0 = 10$ cm. Hence equation (2) gives a value of the slope $s'_{lab} = 85.3$ equivalent to $\theta_{lab} = 89.3°$. This simple scaling analysis was a further justification to use obstacles with vertical sidewalls and we believe that the steep sloping sidewalls of islands do not influence the main results of this study.

7. Conclusions

[40] Laboratory experiments have been performed to investigate the physical processes that govern the interaction of a single vortex with two vertical cylinders. In particular, we are interested in understanding the dynamics that regulate the interaction of a mesoscale vortex with multiple islands, focusing on North Brazil Current (NBC) rings and the Lesser Antilles island chain. The parameters that regulated the flow in the present experiments were the ratio of the gap size to the diameter of the vortex, G/d, and the parameter representing the geometry of the interaction, y/g. Five regimes were observed and the formation of new cyclonic vortices, in the wake of cylinder 1, was observed only for $G/d \leq 0.6$, while formation of new cyclonic vortices, in the wake of both cylinders, was observed only for $0.15 < G/d \leq 0.45$ and $-3 \leq y/g \leq 1$.

[41] However, a third relevant parameter is the relative strength of the vortex compared to the background rotation, i.e., the Rossby number $Ro = \zeta/f$. In the present experiments the value of the Rossby number was not varied and was approximately constant $Ro \approx 0.6-1$. The vortex strength was not varied since it was determined by the technique used to generate the cyclonic vortex. The ice cube positioned in the tank produced a dense plume with an associated low pressure and inward velocities, which are deflected by the Coriolis force to generate an approximately geostrophic cyclonic vortex. To vary the vortex strength, the intensity of the dense plume (i.e., low pressure) has to be varied. Hence withdrawing fluid using of a sink positioned on the sloping bottom and varying the strength of the sink

flow would be a more appropriate method to generate vortices with different strengths. However, we decided to use the simpler apparatus and vortex generation method described in section 2, and vary the parameters discussed above while keeping the vortex strength constant. The outcome of the experiments described in this paper showed such a richness in dynamics that we believe it is important to understand and report first before investigating the importance and effect of varying the vortex strength and, consequently, the Rossby number. We expect that variation of the Rossby number may modify, in particular, the behavior of the interaction of a vortex with a submersed obstacle.

[42] The laboratory model used in the present study is similar to that used by *Cenedese* [2002], and we compared our results with the findings of this previous work that used a single cylinder. The values of the parameters investigated by *Cenedese* [2002] for the present experiments are illustrated in Figure 6, and a comparison of the results with the prediction by *Cenedese* [2002] has been discussed in section 4.

[43] A new and unexpected result was observed for experiments in regime IV. A dipole formed downstream of the passage between the two islands for values of $-2 < y/g < 0$ and $0.25 \leq G/d \leq 0.4$ and provided $Re_G > 200$. The value of the Reynolds number of the fluid from the original vortex funneled through the gap suggests that a dipole will form, if the flow within the gap has a sufficiently high velocity, much like water ejected from a circular nozzle generates a dipole ring. Such value is consistent with previous studies of flow past a right cylinder in a nonrotating and rotating fluid. When considering increasing values of Reynolds number, the flow past a cylinder in a nonrotating environment evolves from laminar potential flow to flow forming two attached vortices in the wake of the cylinder. For values of Reynolds number exceeding about 100, vortices are periodically shed from the cylinder. In the context of rotating environments, a similar qualitative behavior has been observed, with experiments indicating that the critical Reynolds number for vortex shedding is somewhat larger than in the absence of background rotation [*Boyer and Davies*, 1982; *Boyer and Kmetz*, 1983; *Boyer et al.*, 1984]. Hence the values of $Re_G > 200$ observed in the present experiments for dipoles formation are consistent with these previous studies, the only difference being that the uniform flow/jet now instead of going around a single cylinder, it interacts with two halves of a cylinder separated by a gap.

[44] The observation of opposite sign vortices, generated by the interaction of a vortex with multiple islands, has been confirmed in the recent North Brazil Current Ring experiment by Fratantoni and Richardson (submitted manuscript, 2005). Observations of NBC rings interacting with the islands of Saint Vincent and Barbados in the eastern Caribbean revealed the presence of a drifter looping cyclonically (i.e., opposite vorticity than the original NBC ring) downstream of the gap between these two islands (Figure 14a). The passage between the islands of Saint Vincent and Barbados has values of G/d of approximately 0.5; hence the laboratory result suggests that both cyclonic and anticyclonic vortices could form downstream of it.

[45] Finally, we would like to suggest a possible site for dipoles formation and the mechanism of vorticity redistribution discussed in the present paper. The Lesser Antilles is a long chain of islands presenting numerous passages between them having variable width and depth (see Fratantoni and Richardson, submitted manuscript, 2005) (Figure 13). Those passages have values of $0.1 \leq G/d \leq 0.3$ and hence are possible candidates for both cyclonic and anticyclonic vortices formation downstream of them. This hypothetical scenario would give rise to numerous dipoles on the downstream side of the passages, each having a horizontal scale on the order of the passages spacing, i.e., the islands' size [*Linden et al.*, 1995]. If such processes were to occur with NBC rings interacting with the Lesser Antilles, "jetting" through the passages and forming dipole structures downstream of the island chain, how could we reconcile the presence of small vortices of both signs (dipoles) with the large, energetic and predominantly anticyclonic vortices observed by drifters in the eastern Caribbean Sea [*Richardson*, 2005]? Transition from small-scale vortices to large-scale structures can occur by the merging of vortices of like sign. This transfer of energy to larger scales due to coalescence of vortices is a similar process to the well-known feature of inverse energy cascade in two-dimensional flows [e.g., *McWilliams*, 1984]. When rotation is present, the scale to which the vortices grow is determined by instability processes that do not allow vortices to grow to scales larger than the Rossby radius of deformation [*Linden et al.*, 1995]. Hence, if a continuous sequence of vortices was to interact with the island chain, the present experiments suggest that the western side of the islands to be filled with vortices having both cyclonic and anticyclonic vorticity that could merge to give rise to larger vortices in the eastern Caribbean Sea.

[46] Presently there is a lack of information on the fate of the water within the NBC rings "leaking" into the eastern Caribbean via these passages. There is a need for direct observations of the flow through the Lesser Antilles passages in order to determine if dipoles indeed form downstream of the passages or, more in general, if and how the NBC rings' water properties can propagate into the Caribbean Sea. Furthermore, more laboratory and numerical studies are needed to reveal wether the above scenario can be realized. Presently, numerical models (E. Chassignet personal communication) investigating the interaction of NBC rings with the Lesser Antilles did not focus on this particular scenario and a collaborative study linking laboratory, numerical, and observational studies may bring to light important dynamics regulating the fate of the water mass in the NBC rings.

[47] **Acknowledgments.** We wish to thank Jack Whitehead for invaluable discussions, carefully reading drafts and substantially improving the clarity of the manuscript. Support was given by the National Science Foundation project OCE-0081756. The laboratory experiments were carried out with the able assistance of Keith Bradley. Woods Hole Oceanographic Institution contribution 11261.

References

Adduce, C., and C. Cenedese (2004), An experimental study of a monopolar vortex colliding with cylinders of varying geometry in a rotating fluid, *J. Mar. Res.*, *62*, 611–638.

Arhan, M., H. Mercier, and J. R. E. Lutjeharms (1999), The disparate evolution of three Agulhas rings in the South Atlantic Ocean, *J. Geophys. Res.*, *104*, 20,987–21,005.

Boyer, D. L., and P. A. Davies (1982), Flow past a circular cylinder on a β -plane, *Philos. Trans. R. Soc. London, Ser. A*, *306*, 533–556.

Boyer, D. L., and M. K. Kmetz (1983), Vortex shedding in rotating flows, *Geophys. Astrophys. Fluid Dyn.*, *26*, 51–83.

Boyer, D. L., M. K. Kmetz, L. Smathers, G. C. d'Hieres, and H. Didelle (1984), Rotating open channel flow past right circular cylinders, *Geophys. Astrophys. Fluid Dyn.*, *30*, 271–304.

Carton, J. A., and Y. Chao (1999), Caribbean Sea eddies inferred from TOPEX/Poseidon altimetry and a 1/6 Atlantic Ocean model simulation, *J. Geophys. Res.*, *104*, 7743–7752.

Cenedese, C. (2002), Laboratory experiments on mesoscale vortices colliding with a seamount, *J. Geophys. Res.*, *107*(C6), 3053, doi:10.1029/2000JC000599.

Cenedese, C., and J. A. Whitehead (2000), Eddy-shedding from a boundary current around a cape over a sloping bottom, *J. Phys. Oceanogr.*, *30*, 1514–1531.

Csanady, G. T. (1985), A zero potential vorticity model of the North Brazilian Coastal Current, *J. Mar. Res.*, *43*, 553–579.

Cushman-Roisin, B. (1994), *Introduction to Geophysical Fluid Dynamics*, 320 pp., Prentice-Hall, Upper Saddle River, N. J.

Dalziel, S. B. (1992), *DigImage: System Overview*, Cambridge Environ. Res. Consult., Ltd., Cambridge, U. K.

Dewar, W. K. (2002), Baroclinic eddy iInteraction with isolated topography, *J. Phys. Oceanogr.*, *32*, 2789–2805.

Didden, N., and F. Schott (1993), Eddies in the North Brazil Current retroflection region observed by Geosat altimetry, *J. Geophys. Res.*, *98*, 20,120–20,131.

Fratantoni, D. M., and D. A. Glickson (2002), North Brazil Current rings generation and evolution observed with SeaWiFS, *J. Phys. Oceanogr.*, *32*, 1058–1074.

Fratantoni, D. M., W. E. Johns, and T. L. Townsend (1995), Rings of the North Brazil Current: Their structure and behavior inferred from observations and numerical simulations, *J. Geophys. Res.*, *100*, 10,633–10,654.

Fratantoni, D. M., W. E. Johns, T. L. Townsend, and H. E. Hurlburt (2000), Low-latitude circulation and mass transport pathways in a model of the tropical Atlantic Ocean, *J. Phys. Oceanogr.*, *8*, 1944–1966.

Garraffo, Z., W. E. Johns, E. P. Chassignet, and G. J. Goni (2003), North Brazil Current rings and transport of southern waters in a high resolution numerical simulation of the North Atlantic, in *Interhemispheric Water Exchange in the Atlantic Ocean*, *Elsevier Oceanogr. Ser.*, vol. 68, edited by G. J. Goni and P. Malanotte-Rizzoli, pp. 375–409, Elsevier, New York.

Garzoli, S. L., A. Ffield, and Q. Yao (2003), North Brazil Current rings and the variability in the latitude of retroflection, in *Interhemispheric Water Exchange in the Atlantic Ocean*, *Elsevier Oceanogr. Ser.*, vol. 68, edited by G. J. Goni and P. Malanotte-Rizzoli, pp. 357–373, Elsevier, New York.

Goni, G. J., and W. E. Johns (2001), A census of North Brazil Current rings observed from TOPEX/Poseidon altimetry: 1992–1998, *Geophys. Res. Lett.*, *28*, 1–4.

Goni, G. J., and W. E. Johns (2003), Synoptic study of worm rings in the North Brazil Current retroflection region using satellite altimeter data, in *Interhemispheric Water Exchange in the Atlantic Ocean*, *Elsevier Oceanogr. Ser.*, vol. 68, edited by G. J. Goni and P. Malanotte-Rizzoli, pp. 335–356, Elsevier, New York.

Herbette, S., Y. Morel, and M. Arhan (2003), Erosion of a surface by a seamount, *J. Phys. Oceanogr.*, *33*, 1664–1679.

Johns, W. E., T. N. Lee, F. A. Schott, R. J. Zantopp, and R. H. Evans (1990), The North Brazil Current retroflection: Seasonal structure and eddy variability, *J. Geophys. Res.*, *95*, 22,103–22,120.

Kloosterziel, R. C., and G. J. F. van Heijst (1991), An experimental study of unstable barotropic vortices in a rotating fluid, *J. Fluid Mech.*, *223*, 1–24.

Linden, P. F., B. M. Boubnov, and S. B. Dalziel (1995), Source-sink turbulence in a rotating stratified fluid, *J. Fluid Mech.*, *298*, 81–112.

McWilliams, J. C. (1984), The emergence of isolated coherent vortices in turbulent flow, *J. Fluid Mech.*, *146*, 21–43.

Murphy, S. J., H. E. Hurlburt, and J. J. O'Brien (1999), The connectivity of eddy variability in the Caribbean Sea, the Gulf of Mexico, and the Atlantic Ocean, *J. Geophys. Res.*, *104*, 1431–1453.

Ou, H. W., and W. P. DeRuijter (1986), Separation of an inertial boundary current from a curved coastline, *J. Phys. Oceanogr.*, *16*, 280–289.

Pedlosky, J., and M. Spall (1999), Rossby normal modes in basins with barriers, *J. Phys. Oceanogr.*, *29*, 2332–2349.

Pratt, L. J., and M. A. Spall (2003), A porous-medium theory for barotropic flow through ridges and archipelagos, *J. Phys. Oceanogr.*, *33*, 2702–2718.

Richardson, P. L. (2005), Caribbean Current and eddies as observed by surface drifters, *Deep Sea Res., Part II*, *52*, 429–463.

Richardson, P. L., and A. Tychensky (1998), Meddy trajectories in the Canary Basin measured during the SEMAPHORE experiment, 1993–1995, *J. Geophys. Res.*, *103*, 25,029–25,045.

Richardson, P. L., G. E. Huffort, R. Limeburner, and W. S. Brown (1994), North Brazil Current retroflection eddies, *J. Geophys. Res.*, *99*, 5081–5093.

Richardson, P. L., A. S. Bower, and W. Zenk (2000), A census of Meddies tracked by floats, *Progr. Oceanogr.*, *45*, 209–250.

Schouten, M. W., W. P. M. De Ruijter, P. J. Van Leeuwen, and J. R. E. Lutjeharms (2000), Translation, decay and splitting of Agulhas rings in the southeastern Atlantic Ocean, *J. Geophys. Res.*, *105*, 21,913–21,925.

Shapiro, G. I., S. L. Meschanov, and M. V. Emelianov (1992), Mediterranean water lens after a collision with seamounts, *Oceanology*, *32*(3), 279–283.

Shapiro, G. I., S. L. Meschanov, and M. V. Emelianov (1995), Mediterranean lens "Irving" after its collision with seamounts, *Oceanol. Acta*, *18*(3), 309–318.

Simmons, H. L., and D. Nof (2000), Islands as eddy splitters, *J. Mar. Res.*, *58*, 919–956.

Simmons, H. L., and D. Nof (2002), The squeezing of eddies through gaps, *J. Phys. Oceanogr.*, *32*, 314–335.

Van Dyke, M. (1982), *An Album of Fluid Motion*, Parabolic Press, 174 pp., Stanford, Calif.

Wang, G., and W. K. Dewar (2003), Meddy-seamount interactions: Implications for the Mediterranean Salt Tongue, *J. Phys. Oceanogr.*, *33*, 2446–2461.

Whitehead, J. A., M. E. Stern, G. R. Flierl, and B. A. Klinger (1990), Experimental observations of baroclinic eddies on a sloping bottom, *J. Geophys. Res.*, *95*, 9585–9610.

Zhurbas, V., and I. S. Oh (2004), Drifter-derived maps of lateral diffusivity in the Pacific and Atlantic oceans in relation to surface circulation patterns, *J. Geophys. Res.*, *109*, C05015, doi:10.1029/2003JC002241.

C. Adduce, Dipartimento di Scienze dell'Ingegneria Civile, Università di Roma "RomaTre," Rome, Italy.

C. Cenedese and D. M. Fratantoni, Department of Physical Oceanography, Woods Hole Oceanographic Institution, MS 21, Woods Hole, MA 02543, USA. (ccenedese@whoi.edu)